

Nanostructured lipid carriers to enhance transdermal delivery and efficacy of diclofenac

Chien Ngoc Nguyen^{1,2} · Thi Thuy Trang Nguyen¹ · Hanh Thuy Nguyen^{1,3} · Tuan Hiep Tran^{4,5}

Published online: 3 August 2017
© Controlled Release Society 2017

Abstract Lipid carrier-mediated transdermal drug delivery offers several advantages because it is non-irritating and non-toxic, provides effective control of drug release, and forms an adhesive film that hydrates the outer skin layers. However, to penetrate the deeper skin layers, these formulations need to overcome several barriers in the stratum corneum. This study evaluates factors influencing particle size and drug-loading capacity, which play a key role in drug permeation and efficacy. Diclofenac sodium was chosen as the model drug. The fabrication of diclofenac sodium-loaded lipid nanoparticles was optimized by modulating several parameters, including the lipids and surfactants employed, the drug/lipid ratio, and the pH of the aqueous phase. The physical properties and loading efficiencies of the nanoparticles were characterized. The optimized formulation was then dispersed into a polymer solution to form a gel, which demonstrated a sustained *ex vivo* permeation of diclofenac

sodium over 24 h through excised rat skin and a higher drug penetrating capacity than that of a commercially available gel. *In vivo* anti-inflammatory activity was assessed in a rat carrageenan-induced paw edema model; the anti-edema effects of the prepared gel and commercially available gel over 24 h were comparable. The present findings indicate the effects of particle size and drug loading on the ability of nanostructured lipid carrier preparations to provide transdermal drug delivery.

Keywords Transdermal drug delivery · Diclofenac sodium · Lipid carriers · Particle size

Introduction

Diclofenac sodium (DCF) is a well-known non-steroidal anti-inflammatory drug with anti-inflammatory and analgesic activities that is used to treat acute pain and a broad range of inflammatory conditions, including arthritis [1]. The biological half-life of DCF is only 1–2 h because of extensive metabolism in the liver, which necessitates a high dosing frequency [2]. However, DCF has been reported to induce gastrointestinal side effects such as bleeding, ulceration, or perforation of the intestinal wall [3]. Controlled transdermal drug delivery is thus considered to provide an ideal administration route for DCF because it offers several advantages over oral or injected administrations, including avoidance of first-pass metabolism, minimization of pain, and the potential for sustained drug release [4, 5].

In practice, transdermal drug delivery is still limited by the robust nature of the skin. The layers of the skin protect the body from threats in the outer environment, including microorganisms and other environmental stressors such as heat, chemicals, toxicants, and dehydration [6]. Based on a

✉ Chien Ngoc Nguyen
nguyennocchien@yahoo.com

✉ Tuan Hiep Tran
trantuanhiep@tdt.edu.vn

¹ National Institute of Pharmaceutical Technology, Hanoi University of Pharmacy, 13-15 Le Thanh Tong, Hoan Kiem, Ha Noi, Vietnam

² Department of Pharmaceutical Industry, Hanoi University of Pharmacy, Hanoi, Vietnam

³ College of Pharmacy, Yeungnam University, 214-1, Dae-Dong, Gyeongsan 712-749, South Korea

⁴ Department for Management of Science and Technology Development, Ton Duc Thang University, Ho Chi Minh City, Vietnam

⁵ Faculty of Pharmacy, Ton Duc Thang University, Ho Chi Minh City, Vietnam

comprehensive understanding of the skin, researchers have aimed to overcome this barrier and provide topical transdermal drug delivery systems. Lipid nanoparticles provide one of the most promising strategies in this context [7, 8]. The smaller size of lipid nanocarriers may provide a higher specific surface area for drug absorption through the skin, resulting in greater efficacy [9]. Moreover, the occlusive effect of film formation on the skin surface reduces transepidermal water loss, which enhances the penetration of drugs through the stratum corneum [10]. Regarding the effect of particle size on transdermal delivery, Verma et al. investigated liposomes with diameters of 120, 191, 377, and 810 nm and found that smaller particles accumulate in the skin more than larger particles [11]. Sakeel et al. also reported that smaller particles augment drug delivery using nanoemulsions with a size range of 35–68 nm [12]. In another study using the same carboxylate-based nanoparticles, Kohli et al. investigated the performance of 50- to 500-nm particles. Their interesting findings indicate that 50-nm particles initially deliver a high level of drug, whereas 500-nm particles produce superior drug delivery at later time-points [13]. Taken together, these findings indicate that the impact of particle size on transdermal drug delivery is complex and depends on anatomical and physiological characteristics.

DCF-loaded lipid nanoparticles have been developed and characterized as transdermal carriers [2, 14, 15]; however, the means by which the physical properties of the nanoparticle effect treatment efficacy have not yet been fully elucidated. Therefore, the present study aimed to fabricate DCF-loaded nanostructured lipid carriers (NLCs) and DCF-NLC gels for topical application and to observe their transdermal performance *in vitro* and *in vivo*. These formulations were characterized in terms of their particle size and the factors affecting this feature, including the lipid and surfactant employed, the concentration of surfactant and drug, and the pH of the water-dispersed phase. The subsequent *in vitro* and *in vivo* studies of each formulation were conducted to assess the effects of the particle properties on efficacy.

Materials and methods

Materials

All chemicals were used without further purification and obtained from the following commercial sources: DCF (Dongtai Pharm Co. Ltd., Henan, China); glyceryl monostearate (GMS) and lanolin PEG-75 (Sao Thai Duong Co., Viet Nam); Phospholipon® 90G (Phospholipids GmbH, Ludwigshafen, Germany); glyceryl palmito-stearate (Precirol® ATO 5) (Gattefossé, St-Priest, France); polysorbate (Tween 80; Duskan Chemical Co., Ansan, Korea); cremophor RH 40 (BASF, Ludwigshafen, Germany); polyvinyl alcohol

(Kuraray Co. Ltd., Singapore); carboxymethyl cellulose sodium (Daicel Co. Ltd., Japan); cetyl alcohol, cetostearyl alcohol, propylene glycol, and hydroxypropyl cellulose (Zhejiang Kehong Chemical Co., China); carbopol 934 (Cb 934) (Lubrizol, USA); and glycerin (Shanghai Demand Chemical Co. Ltd., Japan). Methanol was of high-performance liquid chromatography (HPLC) grade. Other chemicals were of analytical grade.

Preparation of DCF-loaded NLCs

NLCs were produced using hot homogenization followed by ultra-sonication, as described by Teeranachaideekul et al. [16], with some modification. First, DCF, phospholipids, and lipids were dissolved in an organic solvent mixture of dichloromethane:methanol (6:2, v/v). The mixture was then evaporated using a rotary evaporator (Rotavapor® R-100, Buchi, USA) to obtain a lipid phase. After melting at 70 °C, the lipid phase was dispersed in a hot surfactant solution (70 °C) to obtain an emulsion using a probe sonicator (Vibracell VCX130, Sonics, USA) at an input power of 100 W for 10 min. The temperature was maintained at 70–80 °C during the emulsion process. The lipid dispersion was cooled to room temperature (25 °C) under ambient conditions and solidified to form aqueous NLC dispersions. Each formulation was fabricated in a total volume of 50 mL. The detailed compositions and conditions used are summarized in Table 1.

Lyophilization of the NLC dispersion was carried out in a freeze dryer (FDA5518; IIShin, South Korea) using mannitol (5%, w/v) as the cryoprotectant. The dispersion was pre-frozen (–80 °C) for 12 h prior to lyophilization at –25 °C for 24 h, followed by a 12-h secondary drying phase at 20 °C.

Preparation of gel formulations

NLCs were introduced into hydrogels using carboxymethyl cellulose sodium, hydroxypropyl cellulose, or carbopol 934 as the excipients, and propylene glycol and glycerin as the permeability enhancers [17]. Batches of hydrogel formulations (50 g) were fabricated by adding DCF-loaded NLC suspensions to an aqueous dispersion containing hydrophilic polymer (0.6% carboxymethyl cellulose sodium, 0.3% Cb 934, and 6% hydroxypropyl cellulose) and permeability enhancer (5% of the total volume). Hydrogels were gently stirred overnight and then stored at 4 °C until use.

Characterization of formulations

Determination of particle size and morphology

The samples were diluted tenfold in distilled water prior to measuring the particle size and size distribution by dynamic

Table 1 NLC formulations

Formulation	Oil phase		Aqueous phase			Variable
	Lipid	DCF	P90G	Surfactant	pH	
F1	1.5 g ACA	0.25 g	0.5 g	0.5 g T80	6.1	Lipid
F2	1.5 g CA					
F3	1.5 g Pre					
F4	1.5 g GMS					
F4	1.5 g GMS	0.25 g	0.5 g	0.5 g T80	6.1	Surfactant
F5				0.5 g PVA		
F6				0.5 g Lan-PEG		
F7				0.5 g CreRH		
F8	1.5 g GMS	0.25 g	0.5 g	0 g T80 (0%)	6.1	T80
F4				0.5 g T80 (1%)		
F9				1.0 g T80 (2%)		
F10				1.5 g T80 (3%)		
F11	1.5 g GMS	0.25 g	0 g (0%)	1.0 g T80 (2%)	6.1	P90G
F12			0.1 g (0.2%)			
F13			0.3 g (0.6%)			
F9			0.5 g (1%)			
F14	1.5 g GMS	0.50 g	0.3	1.0 g T80 (2%)	6.1	DCF
F13		0.25 g				
F15		0.15 g				
F16		0.10 g				
F13	1.5 g GMS	0.25 g	0.3	1.0 g T80 (2%)	6.1	pH
F17					4	
F18					3	
F19					2.5	

GMS glyceryl monostearate, DCF diclofenac, T80 Tween 80, Pre Precirol® ATO 5, CA cetyl alcohol, ACA cetostearyl alcohol, P90G Phospholipon® 90G, PVA polyvinyl alcohol, CreRH cremophor RH40, Lan-PEG lanolin PEG-75

laser light scattering on a Zetasizer Nano ZS (Malvern Instruments, UK). The analysis was performed at a scattering angle of 90° and a temperature of 25 °C. These measurements were performed in triplicate.

The morphology of DCF-NLCs was observed using transmission electron microscopy (Hitachi 7600, Japan). For sample preparation, the DCF-NLC suspension was deposited onto the surface of a copper grid (mesh size of 300) coated with carbon, negative-stained with 2% phosphotungstic acid (*w/v*), and then air-dried for 15 min before visualization.

Determination of encapsulation efficiency and drug loading

The drug entrapment efficiency of DCF-NLC was indirectly determined by assaying free DCF in the dispersion medium. The lipid dispersion (2 mL) was loaded into a Millipore UFC801008 Amicon® filter (Amicon Ultra, Millipore, USA) with a molecular weight cutoff of 10 kDa and centrifuged at 4000 rpm for 60 min. Unbound DCF, which moved across the filter membrane to the bottom compartment, was

assayed and the drug entrapment efficiency was then calculated using the following equation:

Entrapment efficiency (%)

$$= \frac{(W_{\text{initial drug}} - W_{\text{unbound drug}})}{W_{\text{initial drug}}} \times 100,$$

where *W* represents the weight in milligrams.

DCF was assayed chromatographically using an Agilent Infinity 1260 HPLC system and a C18 analytical column (Zorbax Eclipse XBD C18; 250 × 4.6 mm, 5 μm; Agilent, Japan) at ambient temperature. The mobile phase comprised methanol and phosphate-buffered solution at pH 2.5 (80:20, *v/v*). The flow rate was 1.0 mL/min, the injection volume was 20 μL, and the effluent was monitored at 254 nm.

Physical characterization of DCF-NLCs

A differential scanning calorimeter (Q-2000; TA, DE, USA) was used to analyze the thermal properties of GMS, DCF, blank NLCs, and DCF-NLCs. Samples were weighed in

standard open aluminum pans using an identical empty pan as the reference. The samples were heated from 40 to 320 °C at 10 °C/min with a nitrogen purge at a flow of 50 mL/min.

Powder X-ray diffraction analysis was performed on GMS, DCF, lyophilized blank NLCs, and DCF-NLCs using a panalytical diffractometer (PANalytical, Almelo, The Netherlands) with Cu K α radiation ($\lambda = 1.54060$) at 40 kV and 30 mA between 10 and 50° (2θ) at room temperature, with a step size of 0.02° and a scan speed of 1°/min.

In vitro release and in vitro/ex vivo permeation studies

In vitro drug release was determined over a period of 24 h using a cellulose acetate synthetic membrane with a molecular weight cutoff of 12 kDa (Sigma-Aldrich, Missouri, USA). The studies were carried out using static Franz diffusion cells (Hanson Research, CA, USA) with a diffusion area of 1.767 cm² and a receptor compartment containing 7 mL phosphate-buffered saline at pH 7.4 [18]. This receptor phase was stirred at 400 rpm and maintained at 37 ± 0.5 °C via a thermostatic water pump, which circulated water through each chamber jacket. Each sample contained an equivalent amount of drug (2 mg), and at pre-determined time-points, 1-mL aliquots were removed and replaced with fresh medium. All DCF concentrations were assayed using the HPLC method described above.

Ex vivo permeation studies were also performed in static Franz diffusion cells (as described above) using the male rat epidermis as a skin model; this was clamped between the donor and receptor compartments with the stratum corneum side facing up [9]. The rat skin was treated as described previously [19, 20] and with the permission of the Ethic Commitment Jury. The fur and lipids were removed from the skin. Intact skin specimens were rinsed in 0.9% saline and covered with aluminum foil prior to storage at -20 °C. Prior to the experiments, the skin was warmed to room temperature; the lower face of the skin was then immersed in a 0.9% saline solution or release media for 30 min.

We measured the concentration of drug retained in the skin after the permeability studies. The drug was extracted into ethanol by means of sonication and centrifugation. Specifically, the skin was rinsed thrice with saline buffer (pH 7.4) and then broken into small pieces and placed into a 10-mL volumetric flask. After adding 5 mL ethanol, the samples were sonicated twice for 30 min each time. The collected solutions were centrifuged at 8000 rpm for 10 min, then filtrated through a 0.45- μ m membrane before being assayed via HPLC [21].

In vivo edema inhibition study

The anti-inflammatory activity of NLC gels was determined using a carrageenan-induced rat paw edema model [20]. The

study protocol was approved by the Ethics Committee of Medicine and Pharmacy Research, Military Medical University (Hanoi, Vietnam, approval number 06C2015). The animals were kept under standard laboratory conditions (temperature, 25 ± 2 °C; relative humidity, 55 ± 5%) and fed a standard laboratory diet.

Forty male rats (8–10 weeks old, with an average weight of 250–280 g) were randomly divided into five groups. Group I (negative control) received gel without drug, whereas group II (positive control) received a commercial product (Voltaren Emulgel; Vol). Groups III, IV, and V were administered Gel 1, Gel 2, or Gel 3 formulations (gels prepared using different types of NLCs), respectively, with the amount of gel being equivalent to 4 mg of DCF. A 1% carrageenan suspension in saline (0.05 mL) was injected into the plantar side of the right hind paw of each rat. The indicated treatments were applied to the plantar surface of the left hind paw, with a cover to avoid drug loss, 0.5 h before the carrageenan injection. The paw volumes were measured prior to treatment and subsequently at 1, 3, 5, 7, and 24 h after the carrageenan injection using a digital plethysmometer model LE 7500 (Letica, Scientific Instruments, Barcelona). Specifically, the treated paw was immersed in water within the measurement chamber. The numbers displayed indicating paw volume, edema rate, and percentage of edema inhibition were calculated using the following formulae [22]:

$$\text{Edema rate (\%)} = \left[(V_t - V_0) / V_0 \right] \times 100$$

$$\text{Edema inhibition (\%)} = \left[(X_c - X_t) / X_c \right] \times 100,$$

where V_0 is the paw volume before the carrageenan injection (mL), V_t is the paw volume at t h after the carrageenan injection (mL), X_c is the edema rate of the control group, and X_t is the edema rate of the treatment group.

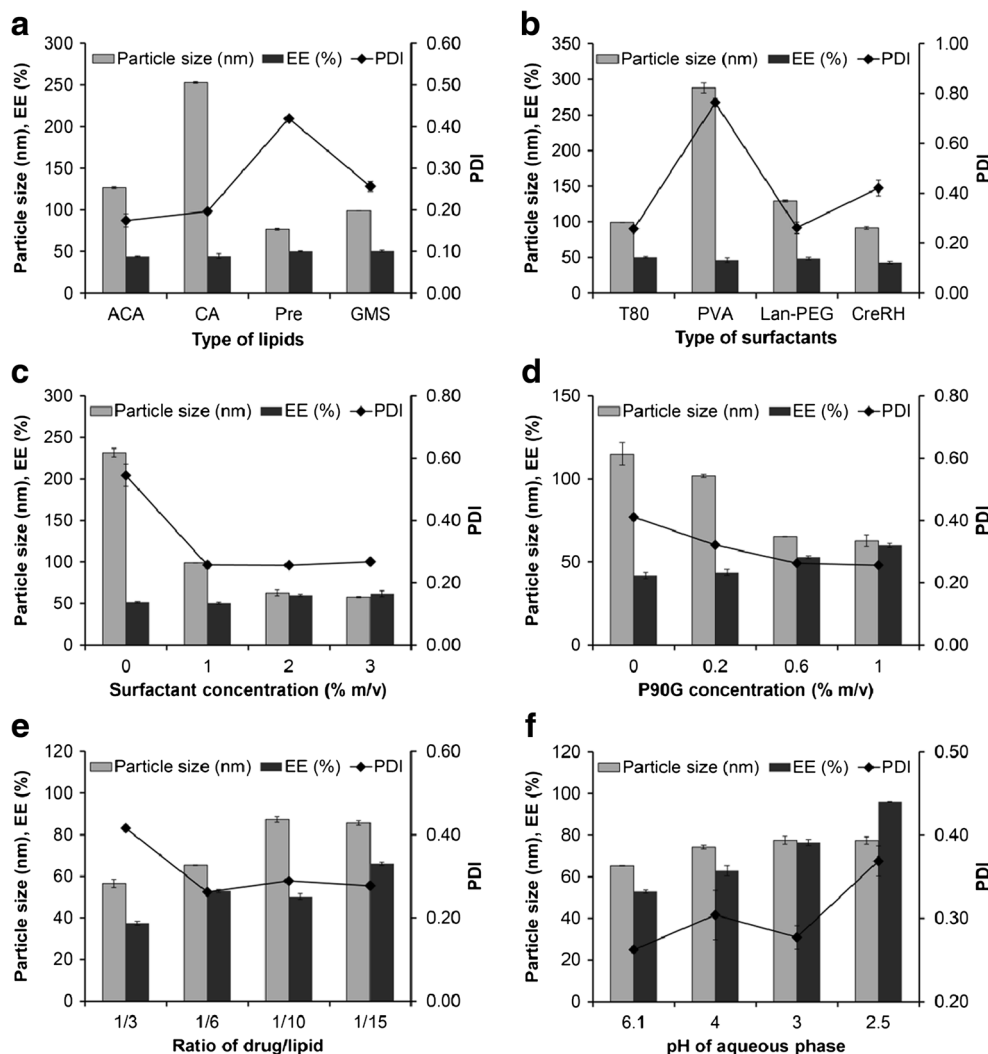
Data are reported as the means ± standard deviation for eight animals per group. Statistical analyses were performed using IBM SPSS Statistics 20.0 software. One-way analysis of variance was employed, followed by Dunnett's T3 post-hoc test for multiple comparisons. p values <0.05 were considered statistically significant.

Results and discussion

Preparation of DCF-NLCs

It is known that the composition of transdermal drug delivery systems has a strong influence on their performance. Thus, this study carefully investigated these influences. Figure 1a shows a narrow size distribution of 100–250 nm for the lipid-based formulation and a low drug-loading capacity, whereas the glyceride-based formulations (GMS, Precirol®,

Fig. 1 Effects of the indicated variables on particle size, polydispersity index (PDI), and drug entrapment efficiency of nanostructured lipid carriers (NLCs) are shown. Data represent the means \pm standard deviation ($n = 3$). CA cetyl alcohol, ACA cetostearyl alcohol, *Pre* Precirol® ATO, *GMS* glyceryl monostearate, *T80* Tween 80, *PVA* polyvinyl alcohol, *Lan-PEG* lanolin PEG-75, *CreRH* cremophor RH 40, *P90G* Phospholipon® 90G



approximately 100 nm) had a reasonably good loading capacity (>50%). This could be attributable to the lower crystallinity of *GMS* or *Precirol*®, leaving more space to accommodate drug molecules [23]. *GMS* was selected for the lipid core based on its narrow size distribution (polydispersity index of 0.26 ± 0.01) and favorable properties; these included a low melting point and well-characterized emulsifying ability [20]. In this study, several surfactants were used to evaluate their effects on carrier properties. Tween 80 was identified as the best choice because of its association with a small particle size, narrow size distribution, and good drug-loading capacity (Fig. 1b). In addition, the mean particle size was reduced by increasing the surfactant concentration, attributable to its surface-active properties in colloidal dispersions [24]. Thus, the concentration of Tween 80 was considered during screening, indicating an optimal concentration of 2% (*w/v*). It is best to use a combination of hydrophobic and hydrophilic surfactants when fabricating emulsions. Therefore, Phospholipon® 90G, a type of phosphatidylcholine, was introduced as a lipophilic

surfactant. A suitable concentration of Phospholipon® 90G forms a single layer on the lipid particle surface and improves the stability of the colloidal system [25]. Moreover, it forms micelles that remain inside the lipid core and increase the drug-loading capacity. Our data show that the desired particles were obtained using 0.6% *w/v* Phospholipon® 90G (Fig. 1d).

High drug-loading capacity is an important criterion for drug delivery systems. To optimize this, the drug/lipid ratio and pH of the aqueous phase was investigated. The drug entrapment efficiency and loading capacity were enhanced when the drug/lipid ratio and pH were reduced, which is understandable considering that a higher amount of lipid provides more space for drug accommodation. DCF is a pH-dependent drug, with a *pKa* of about 4; therefore, the drug will exist in a hydrophobic state at a low pH and can be dissolved more readily into the organic phase, resulting in a higher loading capacity (Fig. 1f) [26]. The optimized formulation, which was used for further characterizations, contained 3% *GMS*, 2% Tween 80, 0.6% Phospholipon® 90G, and an external phase

Table 2 Compositions and properties of the optimized formulations

	GMS (% w/v)	DCF (% w/v)	T80 (% w/v)	P90G (% w/v)	Size (nm)	Polydispersity index	Entrapment efficiency (%)
NLC 1	3	0.5	2	0.6	54.38 ± 1.54	0.250 ± 0.009	60.67 ± 0.30
NLC 2	6	0.4	2	1.2	126.67 ± 1.21	0.259 ± 0.004	76.42 ± 4.06
NLC 3	3	0.2	2	0.6	92.75 ± 0.82	0.305 ± 0.008	78.26 ± 0.65

GMS glyceryl monostearate, DCF diclofenac, T80 Tween 80, P90G Phospholipon® 90G

pH of 3 (F18). Under these conditions, three different formulations (NLC 1–3) were fabricated (Table 2) and details regarding their properties elucidated.

Characterization of DCF-NLCs

Transmission electron microscopy images of DCF-NLCs were captured to observe morphology. Figure 2 clearly shows that DCF-NLCs were spherical, with a nanometric size range and a narrow size distribution. The particle sizes of NLC 1, NLC 2, and NLC 3 were approximately 50, 150, and 100 nm, respectively, which is consistent with the corresponding dynamic light scattering data.

Differential scanning calorimetric thermograms of bulk GMS, pure DCF, lyophilized blank NLCs, and DCF-NLCs are displayed in Fig. 3a. The thermograms of pure DCF and GMS show sharp endothermic peaks at 297.4 and 63.7 °C, respectively, indicating their melting points. However, the DCF melting point was absent from the DCF-NLC thermogram, indicating that DCF had either transformed from a crystalline to amorphous state or had dispersed within the lipid matrix in the molecular state [27]. In contrast, a reduction in GMS peak intensity indicated a decrease in the degree of crystallinity of the NLC lipid matrix. This phenomenon shows the potential for expanding the drug-loading capacity [28]. The X-ray diffraction data also identified sharp crystalline peaks in pure DCF at 15.00, 17.00, 19.7, and 27.74; these

peaks disappeared when the drug was incorporated into the formulation. The intensity of the GMS peak was also lower for the NLC formulation than that for the pure form (Fig. 3b).

Preparation of gel formulations

Although optimized NLCs were identified, their low viscosity and adhesion meant that they are inadequate for transdermal administration. Therefore, the addition of hydrophilic polymers is required, and their impact on system properties, including appearance, gel state, and drug release, need to be evaluated [29]. In our study, the gels were first prepared using polymers (carboxymethyl cellulose sodium, Cb 934, and hydroxypropyl cellulose). As shown in Fig. 4a, the drug release profiles for all formulations were similar after 24 h, with approximately 30% of the drug released. However, only the Cb 934 formulation was observed to have a homogenous appearance. Gels were then formulated with Cb 934 concentrations of 0.3–0.5% using triethylamine to adjust the pH to 6–7. Cb 934 has a concentration-dependent influence on gel viscosity, which reportedly modulates the dissolution rate by which higher polymer concentrations reduce the release of drug [30]. Therefore, a formulation containing 0.3% Cb 934 was selected because of its high drug dissolution rate (>50% after 24 h). To improve this rate, a permeability enhancer was added. At a concentration of 5% total volume, propylene glycol significantly increased drug release to 64.9% after 24 h,

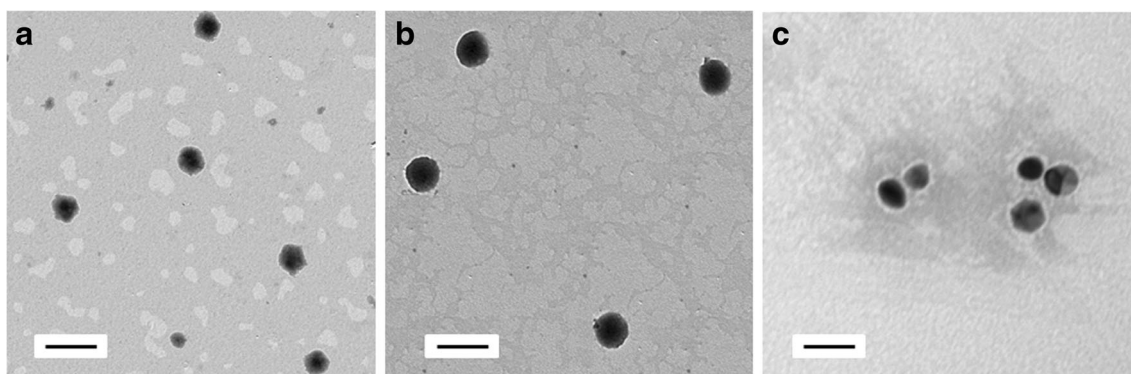


Fig. 2 Transmission electron micrographs of diclofenac sodium nanostructured lipid carriers (DCF-NLCs). **a** NLC 1, **b** NLC 2, and **c** NLC 3 are shown. Bar = 200 nm

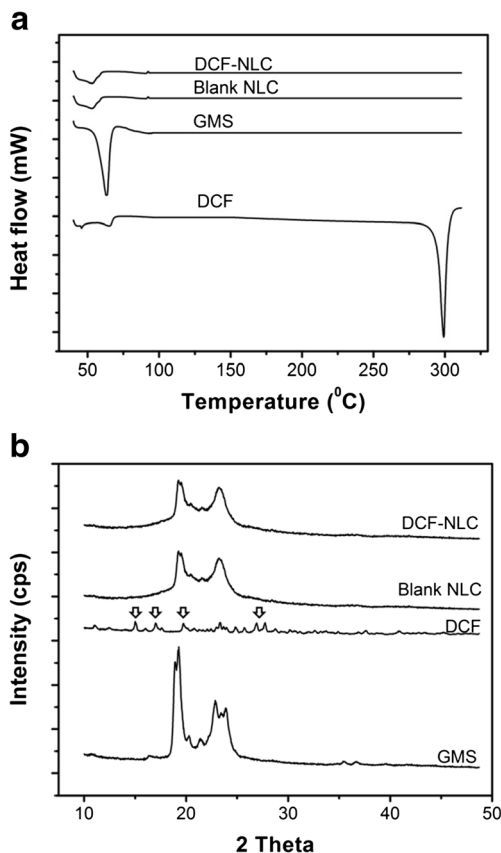


Fig. 3 Physical characterizations of diclofenac sodium (DCF), glyceryl monostearate (GMS), blank nanostructured lipid carriers (NLCs), and DCF-NLC. **a** Differential scanning calorimetric thermograms and **b** X-ray diffraction patterns are shown. The characteristic peaks of DCF are noted with an *arrow*

whereas glycerin did not change this property significantly (Fig. 4c). Thus, propylene glycol and Cb 934 were chosen to formulate the carriers used in subsequent tests.

Ex vivo skin permeation study

Skin permeation profiles of the gel formulations were characterized ex vivo. This study was conducted using three different NLC systems, with the component ratios and properties detailed in Table 2. The results displayed in Fig. 5 clearly indicate the effects of particle size and drug loading on drug delivery. The cumulative amounts of permeated drug after 24 h differed significantly between the NLC samples ($p < 0.05$); these were 448.77 ± 23.77 , 347.39 ± 9.68 , and $177.14 \pm 39.71 \mu\text{g}/\text{cm}^2$ for NLC 1, NLC 2, and NLC 3, respectively (Fig. 5a). The amount of drug retained in the skin after 24 h (Fig. 5b) was $109.88 \pm 19.04 \mu\text{g}/\text{cm}^2$ for NLC 1, $99.09 \pm 18.64 \mu\text{g}/\text{cm}^2$ for NLC 2, and $82.22 \pm 20.57 \mu\text{g}/\text{cm}^2$ for NLC 3. When comparing the cumulative amounts of permeated drug 24 h after the application of NLC 1 and NLC 3 or of NLC 2 and NLC 3, the role of particle size and/or drug

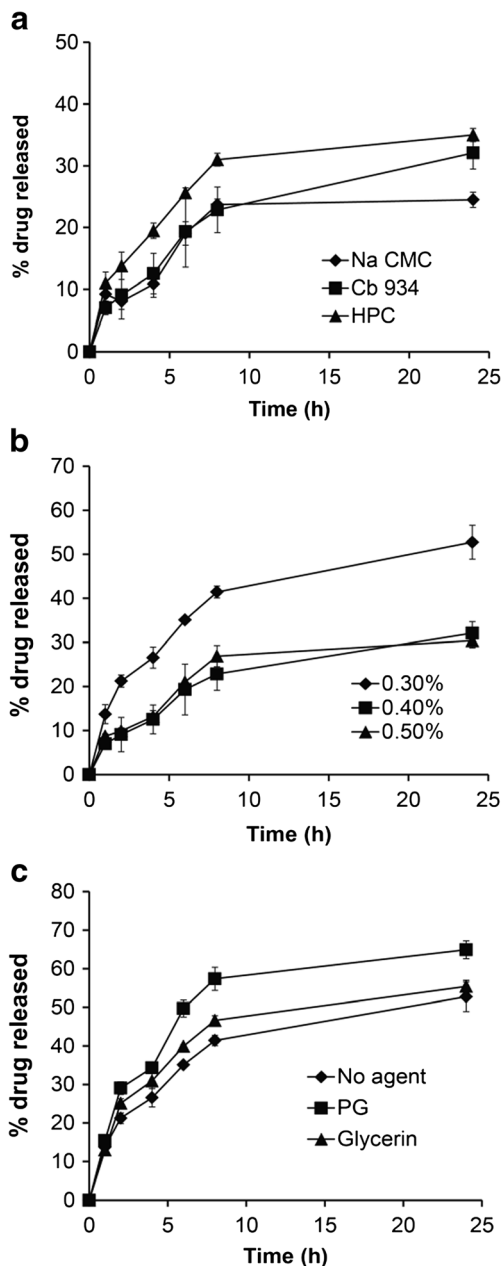
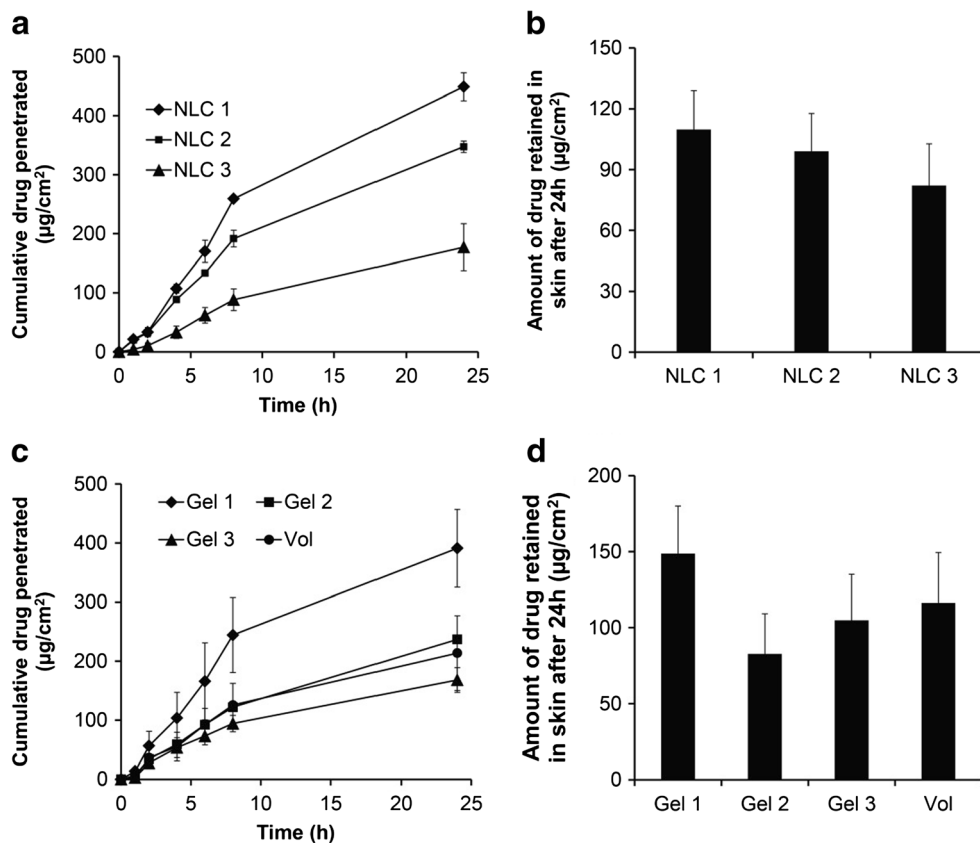


Fig. 4 Effect of gel composition on in vitro drug release. **a** The type of hydrophilic polymer, **b** Cb 934 concentration, and **c** type of enhanced permeability agent are shown. Data represent the means \pm standard deviation ($n = 3$). Cb 934 carbopol 934, Na CMC carboxymethyl cellulose sodium, HPC hydroxypropyl cellulose, PG propylene glycol

loading could be observed after taking the amount of free drug into account. For example, the cumulative amount of permeated drug 24 h after the application of NLC 1 was 153.3% higher than that observed using NLC 3, while the free drug level (calculated from Table 2) was only 80.9% higher for NLC 1 than that for NLC 3. However, when comparing the cumulative amounts of permeated drug 24 h after the application of NLC 1 and NLC 2, we noted that other factors should be considered, such as the concentration of lipid and lipophilic surfactant. With the same lipid concentration, we consistently

Fig. 5 **a, c** Permeation profiles of nanostructured lipid carrier (NLC) dispersions and the respective hydrogels are shown. **b, d** The amount of drug retained in the skin 24 h after administration of NLC dispersions or hydrogels is shown. Data represent the means \pm standard deviation ($n = 3$)



found that a reduction in particle size and increase in drug loading improved drug delivery efficacy by enhancing drug penetration and increasing the amount of the drug retained in the skin. Nevertheless, this phenomenon was not observed clearly in the presence of different lipid concentrations. All three enriched carbopol gel formulations were also investigated in a similar manner. The cumulative amount of permeated drug was highest for Gel 1 at all pre-determined time-points (Fig. 5c) and lowest for Gel 3. Gel 2 and Vol both produced much less drug delivery than Gel 1. At the end of the study (24 h), the amounts of permeated drug were 391 ± 65.84 , 236.89 ± 7.02 , 168.11 ± 20.94 , and 231.53 ± 63.43 $\mu\text{g}/\text{cm}^2$ for Gel 1, Gel 2, Gel 3, and Vol, respectively. Consistent with the trends observed using NLCs, nanoparticle-loaded drug predominated over free drug. The cumulative amount of permeated drug 24 h after the application of Gel 2 was 40.9% higher than that observed for Gel 3, while the free drug of NLC 2 (calculated from Table 2) was only 8.5% higher than that of NLC 3. In addition, the amount of retained drug in the skin 24 h after the application of Gel 1 was also the highest (148.71 ± 31.29 $\mu\text{g}/\text{cm}^2$); the others were in the following order: Vol > Gel 3 > Gel 2. Figure 5 demonstrates that the enriched gel released the drug more slowly than the corresponding intact NLC. This could reflect the increased time required for the drug to be released from the carriers and disperse through the gel matrix to reach the skin; drug released

from NLCs has direct access to the skin [20]. In contrast, the amount of drug retained in the gel was greater than that retained in NLCs, especially for Gel 1. The wettability and adhesion of the hydrophilic polymer (carbopol) may contribute to this enhancement [11]. The stratum corneum is the greatest barrier to transdermal transport. Within the stratum corneum, which comprises a total of 15 layers, the inter-corneocyte space is reported to be only 75 nm wide [31]. This could explain the superiority of the small NLC 1 particles (about 55 nm) over that of the larger NLC particles.

In vivo determination of edema inhibition

As the drug permeability achieved by Gel 1 was much greater than that achieved using the commercial product (Vol), we further investigated this promising product for in vivo anti-inflammatory activity, as evidenced by the inhibition of edema. The data in Table 3 and Fig. 6 clearly show that Gel 1 inhibited edema more than Vol, and the edema inhibition rate increased with particle sizes of <75 nm (Gels 1–3) at 5 and 7 h. For instance, the 5-h inhibition rate of Gel 1 was approximately 72.2%, while Vol, Gel 2, and Gel 3 produced inhibition rates of 67.7, 66.5, and 60.9%, respectively. The edema rates for Gel 1, Vol, Gel 2, and Gel 3 were significantly different from those of the negative control group ($p < 0.05$) at 3, 5, and 7 h. The strongest effect was observed with Gel 1 ($p < 0.01$) at

Table 3 In vivo comparison of the effects on rat carrageenan-induced paw edema

		1 h	3 h	5 h	7 h	24 h
Voltaren Emulgel	X%	4.51 ± 3.17	14.46 ± 1.57 ^b	14.22 ± 7.88 ^a	12.82 ± 9.14 ^a	7.69 ± 4.60
	I%	25.11	40.76	67.69	50.11	35.82
Gel 1	X%	3.51 ± 3.13	10.10 ± 3.99 ^b	12.23 ± 4.29 ^b	9.99 ± 3.60 ^b	6.06 ± 2.68 ^a
	I%	41.72	58.61	72.21	61.13	49.41
Gel 2	X%	3.24 ± 2.83	9.52 ± 8.37 ^b	14.73 ± 7.72 ^a	11.87 ± 5.53 ^b	5.79 ± 2.48 ^a
	I%	46.27	60.99	66.53	53.83	51.65
Gel 3	X%	4.50 ± 2.21	12.50 ± 5.14 ^b	17.20 ± 6.60 ^a	14.03 ± 5.47 ^a	9.11 ± 4.10
	I%	25.32	48.79	60.91	45.42	23.95
Control	X%	6.03 ± 6.88	24.41 ± 4.21	43.99 ± 21.92	25.70 ± 7.71	11.98 ± 5.97

Data are expressed as the mean ± standard deviation

X edema rate, I edema inhibition

^a $p < 0.05$ vs controls

^b $p < 0.01$ vs controls (ANOVA followed by Dunnett's T3 post-hoc test)

these time-points. However, the edema rates observed using Vol, Gel 2, and Gel 3 did not differ significantly at 3, 5, or 7 h ($p > 0.05$). The performance of these gels suggests an influence of other factors. First, there is no doubt that the composition of the formulation influences its physical properties, including particle size, drug loading, and viscosity. As reported in many previous publications, drugs can penetrate through the skin via several routes, including an intercellular pathway through the lipid bilayer, a transcellular pathway through keratin-rich corneocytes, and a shunt pathway through hair follicles and sweat ducts [32]. The stratum corneum pores, which are also potential gateways to deeper skin sites, are estimated to range in size from 20 to 200 nm [33]. Moreover, hydration-mediated expansion of the stratum corneum may increase this size, allowing increased drug penetration and enhancement. Furthermore, penetration enhancers have been reported to induce changes in the hydrocarbon chains of the stratum corneum and lipid components, resulting in increased drug permeation [34]. In addition, surfactant concentration plays an important role in both the fabrication of small particles and in the manipulation of viscosity. The higher the surfactant concentration (in compromise with

viscosity) that is provided, the more drug that is released. Last but not least, the smaller particle sizes provide a larger surface area, resulting in a greater drug release rate. Taken together, Gel 1 should be the one that can converge those criteria in balance to improve DCF performance over the other, especially, commercial product.

Conclusions

The present study was designed to investigate the factors influencing particle size and the effect of particle size and drug loading on transdermal gel characteristics and drug delivery efficacy. After selecting the appropriate components and conditions, NLCs were successfully fabricated and evaluated. A high drug-loading capacity and small particle size ensured a controlled release pattern and good drug permeation. It was noted that higher drug loading was achieved using smaller particles, and that increased drug penetration was associated with greater in vivo efficacy. Furthermore, the resultant optimized gel formulation provided an effective system for the transdermal delivery of DCF.

Acknowledgements We would like to acknowledge the Ethics Committee of Medicine and Pharmacy Research, Military Medical University (Hanoi, Vietnam) for approving our study protocol.

Compliance with ethical standards

Conflict of interest The authors declare that they have no conflict of interest regarding the publication of this paper.

Animal studies All institutional and national guidelines for the care and use of laboratory animals were followed.

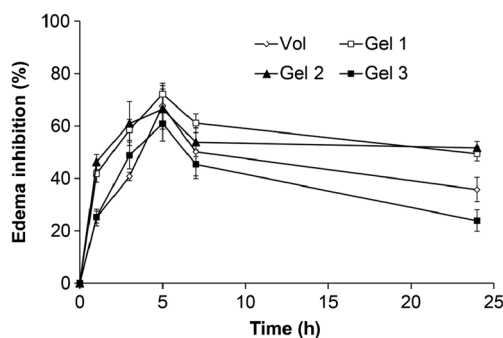


Fig. 6 In vivo edema inhibition study. Data represent means ± standard error ($n = 6$)

References

- Arias JL, López-Viota M, López-Viota J, Delgado ÁV. Development of iron/ethylcellulose (core/shell) nanoparticles loaded with diclofenac sodium for arthritis treatment. *Int J Pharm*. 2009;382:270–6.
- Liu D, Ge Y, Tang Y, Yuan Y, Zhang Q, Li R, Xu Q. Solid lipid nanoparticles for transdermal delivery of diclofenac sodium: preparation, characterization and in vitro studies. *J Microencapsul*. 2010;27:726–34.
- Baraf HS, Fuentealba C, Greenwald M, Brzezicki J, O'Brien K, Soffer B, Polis A, Bird S, Kaur A, Curtis SP, EDGE Study Group. Gastrointestinal side effects of etoricoxib in patients with osteoarthritis: results of the Etoricoxib versus diclofenac sodium gastrointestinal tolerability and effectiveness (EDGE) trial. *J Rheumatol*. 2007;34:408–20.
- Sintov AC, Botner S. Transdermal drug delivery using microemulsion and aqueous systems: influence of skin storage conditions on the in vitro permeability of diclofenac from aqueous vehicle systems. *Int J Pharm*. 2006;311:55–62.
- Gaur PK, Purohit S, Kumar Y, Mishra S, Bhandari A. Preparation, characterization and permeation studies of a nanovesicular system containing diclofenac for transdermal delivery. *Pharm Dev Technol*. 2014;19:48–54.
- Rehman K, Zulfakar MH. Recent advances in gel technologies for topical and transdermal drug delivery. *Drug Dev Ind Pharm*. 2014;40:433–40.
- Schäfer-Korting M, Mehnert W, Korting H-C. Lipid nanoparticles for improved topical application of drugs for skin diseases. *Adv Drug Del Rev*. 2007;59:427–43.
- Cevc G, Vierl U. Nanotechnology and the transdermal route: a state of the art review and critical appraisal. *J Control Release*. 2010;141:277–99.
- Vitorino C, Almeida J, Gonçalves LM, Almeida AJ, Sousa JJ, Pais AACC. Co-encapsulating nanostructured lipid carriers for transdermal application: from experimental design to the molecular detail. *J Control Release*. 2013;167:301–14.
- Bhaskar K, Anbu J, Ravichandiran V, Venkateswarlu V, Rao YM. Lipid nanoparticles for transdermal delivery of flurbiprofen: formulation, in vitro, ex vivo and in vivo studies. *Lipids Health Dis*. 2009;8:1–15.
- Alexander A, Dwivedi S, Ajazuddin, Giri TK, Saraf S, Saraf S, Tripathi DK. Approaches for breaking the barriers of drug permeation through transdermal drug delivery. *J Control Release*. 2012;164:26–40.
- Shakeel F, Baboota S, Ahuja A, Ali J, Aqil M, Shafiq S. Nanoemulsions as vehicles for transdermal delivery of aceclofenac. *AAPS PharmSciTech*. 2007;8:191–9.
- Kohli A, Alpar H. Potential use of nanoparticles for transcutaneous vaccine delivery: effect of particle size and charge. *Int J Pharm*. 2004;275:13–7.
- Fang J-Y, Sung K, Lin H-H, Fang C-L. Transdermal iontophoretic delivery of diclofenac sodium from various polymer formulations: in vitro and in vivo studies. *Int J Pharm*. 1999;178:83–92.
- Özgüney IS, Karasulu HY, Kantarci G, Sözer S, Güneri T, Ertan G. Transdermal delivery of diclofenac sodium through rat skin from various formulations. *AAPS PharmSciTech*. 2006;7:E39–45.
- Teeranachaiideekul V, Souto EB, Junyaprasert VB, Müller RH. Cetyl palmitate-based NLC for topical delivery of coenzyme Q10—development, physicochemical characterization and in vitro release studies. *Eur J Pharm Biopharm*. 2007;67:141–8.
- Puglia C, Blasi P, Rizza L, Schoubben A, Bonina F, Rossi C, Ricci M. Lipid nanoparticles for prolonged topical delivery: an in vitro and in vivo investigation. *Int J Pharm*. 2008;357:295–304.
- Vitorino C, Almeida A, Sousa J, Lamarche I, Gobin P, Marchand S, Couet W, Olivier JC, Pais A. Passive and active strategies for transdermal delivery using co-encapsulating nanostructured lipid carriers: in vitro vs. in vivo studies. *Eur J Pharm Biopharm*. 2014;86:133–44.
- Pillai O, Panchagnula R. Transdermal delivery of insulin from poloxamer gel: ex vivo and in vivo skin permeation studies in rat using iontophoresis and chemical enhancers. *J Control Release*. 2003;89:127–40.
- Gaur PK, Mishra S, Purohit S. Solid lipid nanoparticles of guggul lipid as drug carrier for transdermal drug delivery. *Biomed Res Int*. 2013;2013:750690.
- Gaddam N, Aukunuru J. Systemic delivery of diclofenac sodium after topical application of gels incorporated with drug-loaded solid lipid nanoparticles (SLN). *Asian J Pharm Res Health Care*. 2010;2:177–87.
- Tsai CC, Lin CC. Anti-inflammatory effects of Taiwan folk medicine 'Teng-Khia-U' on carrageenan-and adjuvant-induced paw edema in rats. *J Ethnopharmacol*. 1998;64:85–9.
- Jenning V, Gohla S. Comparison of wax and glyceride solid lipid nanoparticles (SLN®). *Int J Pharm*. 2000;196:219–22.
- Tran TH, Ramasamy T, Cho HJ, Kim YI, Poudel BK, Choi HG, Yong CS, Kim JO. Formulation and optimization of raloxifene-loaded solid lipid nanoparticles to enhance oral bioavailability. *J Nanosci Nanotechnol*. 2014;14:4820–31.
- Schubert M, Müller-Goymann C. Characterisation of surface-modified solid lipid nanoparticles (SLN): influence of lecithin and nonionic emulsifier. *Eur J Pharm Biopharm*. 2005;61:77–86.
- Liu D, Jiang S, Shen H, Qin S, Liu J, Zhang Q, Li R, Xu Q. Diclofenac sodium-loaded solid lipid nanoparticles prepared by emulsion/solvent evaporation method. *J Nanopart Res*. 2011;13:2375–86.
- Tran TH, Ramasamy T, Truong DH, Shin BS, Choi H-G, Yong CS, Yong CS, Kim JO. Development of vorinostat-loaded solid lipid nanoparticles to enhance pharmacokinetics and efficacy against multidrug-resistant cancer cells. *Pharm Res*. 2014;31:1978–88.
- Tran TH, Ramasamy T, Truong DH, Choi H-G, Yong CS, Kim JO. Preparation and characterization of fenofibrate-loaded nanostructured lipid carriers for oral bioavailability enhancement. *AAPS PharmSciTech*. 2014;15:1509–15.
- Souto E, Wissing S, Barbosa C, Müller R. Evaluation of the physical stability of SLN and NLC before and after incorporation into hydrogel formulations. *Eur J Pharm Biopharm*. 2004;58:83–90.
- Cheong LWS, Heng PWS, Wong LF. Relationship between polymer viscosity and drug release from a matrix system. *Pharm Res*. 1992;9:1510–4.
- Cevc G. Lipid vesicles and other colloids as drug carriers on the skin. *Adv Drug Del Rev*. 2004;56:675–711.
- Zakrewsky M, Kumar S, Mitragotri S. Nucleic acid delivery into skin for the treatment of skin disease: proofs-of-concept, potential impact, and remaining challenges. *J Control Release*. 2015;219:445–56.
- Dragicevic N, Maibach HI. Percutaneous penetration enhancers chemical methods in penetration enhancement: drug manipulation strategies and vehicle effects. 2015th ed. Berlin: Springer; 2015.
- Kirjavainen M, Mönkkönen J, Saukkosaari M, Valjakka-Koskela R, Kiesvaara J, Urtti A. Phospholipids affect stratum corneum lipid bilayer fluidity and drug partitioning into the bilayers. *J Control Release*. 1999;58:207–14.